RHEUMATOLOGY

Original article

Targeted photodynamic therapy selectively kills activated fibroblasts in experimental arthritis

Daphne N. Dorst [1,2], Mark Rijpkema[1], Marti Boss[1], Birgitte Walgreen[2], Monique M. A. Helsen[2], Desirée L. Bos[1], Maarten Brom[1], Christian Klein[3], Peter Laverman[1], Peter M. van der Kraan[2], Martin Gotthardt[1], Marije I. Koenders[2] and Mijke Buitinga[4]

Abstract

Objective. In RA, synovial fibroblasts become activated. These cells express fibroblast activation protein (FAP) and contribute to the pathogenesis by producing cytokines, chemokines and proteases. Selective depletion in inflamed joints could therefore constitute a viable treatment option. To this end, we developed and tested a new therapeutic strategy based on the selective destruction of FAP-positive cells by targeted photodynamic therapy (tPDT) using the anti-FAP antibody 28H1 coupled to the photosensitizer IRDye700DX.
Methods. After conjugation of IRDye700DX to 28H1, the immunoreactive binding and specificity of the conjugate were determined. Subsequently, tPDT efficiency was established *in vitro* using a 3T3 cell line stably transfected with FAP. The biodistribution of [^{111}In]In-DTPA-28H1 with and without IRDye700DX was assessed in healthy C57BL/6N mice and in C57BL/6N mice with antigen-induced arthritis. The potential of FAP-tPDT to induce targeted damage was determined *ex vivo* by treating knee joints from C57BL/6N mice with antigen-induced arthritis 24 h after injection of the conjugate. Finally, the effect of FAP-tPDT on arthritis development was determined in mice with collagen-induced arthritis.
Results. 28H1-700DX was able to efficiently induce FAP-specific cell death *in vitro*. Accumulation of the anti-FAP antibody in arthritic knee joints was not affected by conjugation with the photosensitizer. Arthritis development was moderately delayed in mice with collagen-induced arthritis after FAP-tPDT.
Conclusion. Here we demonstrate the feasibility of tPDT to selectively target and kill FAP-positive fibroblasts *in vitro* and modulate arthritis *in vivo* using a mouse model of RA. This approach may have therapeutic potential in (refractory) arthritis.

Key words: fibroblast activation protein, rheumatoid arthritis, photodynamic therapy, collagen induced arthritis

CLINICAL SCIENCE

Rheumatology key message

- FAP-tPDT is feasible in an experimental arthritis model.

Introduction

RA is a chronic, relapsing and remitting inflammatory disease of the synovial joints affecting up to 1% of the population [1]. Progressive damage to both the cartilage and bone in the affected joint, as well as hyperplasia of the synovium are hallmarks of the disease [2]. Immune cells infiltrate the synovium in response to unknown stimuli and subsequently produce a host of cytokines,

---

[1]Department of Radiology and Nuclear Medicine, Radboud University Medical Center, Nijmegen, The Netherlands, [2]Department of Experimental Rheumatology, Radboud University Medical Center, Nijmegen, The Netherlands, [3]Roche Pharmaceutical Research and Early Development, Roche Innovation Center Zurich, Schlieren, Switzerland and [4]Clinical and Experimental Endocrinology, KU Leuven, Leuven, Belgium

chemokines and proteases that aggravate and perpetuate disease. DMARDS are currently used to treat RA. These agents systemically suppress the inflammation, but cause unwanted side effects such as an increased incidence of infections. Furthermore, despite improvement in disease management, a considerable percentage of patients suffer from refractory disease [3].

Fibroblast like synoviocytes (FLS) are thought to play an important role in disease pathogenesis, as demonstrated by their distinct phenotype in inflamed joints, differing from healthy fibroblasts, but also from fibroblasts in other diseases affecting synovial joints, such as OA [4–6]. These differences persist even in the absence of external stimulation [7, 8]. Furthermore, distinct functional subsets of fibroblasts in the lining and sublining layers of the affected synovium have recently been described [9, 10].

Markers of SFs include cadherin-11, CD55, Thy-1, podoplanin and fibroblast activation protein (FAP) [5, 9, 11]. FAP is a cell-surface bound dipeptidyl peptidase with collagenase activity that is abundantly expressed in granulation tissue of healing wounds [12]. Upon activation, SFs upregulate FAP expression and simultaneously adopt a more aggressive phenotype. Levels of FAP expression correlate with inflammation in murine models of arthritis and are elevated in RA synovium compared with the synovium of OA patients [13–15]. Depletion of FAP+ SFs decreased inflammation and ameliorated cartilage destruction in mouse models of arthritis [10, 15]. Specifically targeting FAP+ SFs, while sparing the other SF subsets in affected joints, may thus be an attractive therapeutic strategy for patients with RA [16]. To this end, FAP-targeted photodynamic therapy (tPDT) could be an innovative and elegant approach.

In tPDT, a light-sensitive molecule [a photosensitizer (PS)] is conjugated to a targeting agent [17]. The PS absorbs light of a specific wavelength and may transfer this energy either through the emission of fluorescent light or to molecular oxygen to generate reactive oxygen species (ROS) [18]. These ROS can subsequently damage and destroy the cells that the photosensitizer is bound to.

Here we investigate if targeting activated SFs using FAP-tPDT will induce cell-specific cell death both in cell lines and experimental arthritis in mice. The FAP-targeting antibody 28H1 is conjugated to the PS IRDye700DX as well as with diethylenetriaminepentaacetic acid (DTPA) for radiolabelling with ^{111}In, resulting in the tracer [^{111}In]In-DTPA-28H1-700DX. We demonstrate the efficacy of this compound for tPDT in FAP-expressing cells. Furthermore, we assess the biodistribution of the compound in mice with antigen-induced arthritis (AIA) as well as its feasibility and therapeutic potential in CIA.

Methods

Animals

Female C57BL/6NRj and male DBA/1JRj mice were obtained from Janvier-Elevage (Le Genest-Saint-Isle,

France). All mice were housed in individually ventilated cages under specific pathogen-free conditions. The animals were fed standard chow *ad libitum* and housed on a 12 h day-night cycle. The mice were used at between 10 and 12 weeks of age. The Radboud University animal ethics committee approved the study protocol (RU-DEC-2016-0076, CCD number AVD103002016786). All procedures were performed according to the Institute of Laboratory Animal Research Guide for Laboratory Animals.

Antibody conjugation and radiolabelling

For this study the human IgG1 anti-human/mouse FAP antibody 28H1 was used as described previously [13, 19]. It has a high pM avidity for both murine (<1 pM) and human (268 pM) FAP and bears a P329G LALA mutated Fc part, preventing activation of Fcγ receptors [20]. The antibody was conjugated to the photosensitizer IRDye700DX (Li-cor, Lincoln, NB, USA) using an -N-hydroxysuccinimidyl ester. Briefly, the antibody was incubated with a 3–10 M excess of IRDye700DX in 10% w/v 1 M NaHCO$_3$ (pH 8.5) at room temperature for 1 h. Additionally a p-isothiocyanatobenzyl DTPA [ITC-DTPA (Macrocyclics, Plano, TX, USA)] chelator was conjugated to the construct by incubation of a 10-fold molar excess of the chelator in 10% w/v 1 M NaHCO$_3$ (pH 9.5) at room temperature for 1 h. A control conjugate with only DTPA was also made using a 10-fold molar excess of ITC-DTPA, as described above. Free IRDye700DX and ITC-DTPA were removed through dialysis with a Slide-A-Lyzer Dialysis Cassette (20.000 MWCO, Thermo Fisher, Waltham, MA, USA) in PBS with 0.5% w/v Chelex (Bio-Rad, Hercules, CA, USA). The antibody conjugate was stored in PBS at 4°C for a maximum of 3 months. To determine the concentration, optical density measurements were performed. Absorbance was measured at 280 nm for protein and 689 nm for the PS using the Infinite M200Pro Tecan system (Tecan, Männedorf, Switzerland). The number of PSs per antibody molecule [the substitution ratio (SR)] was estimated using the optical density, extinction coefficients and approximate molecular weights of the different components (150 kDa for the antibody and 1954 Da for the PS). By adding different molar excess concentrations of IRDye700DX ranging from 3 to 10, an SR ranging from 1.2 to 7.5 PS molecules per antibody could be obtained. Labelling with ^{111}InCl$_3$ (Covidien, Petten, The Netherlands) was performed as described previously [13, 21]. Radiochemical purity was >99% for both DTPA-28H1-700DX and DTPA-28H1 as determined by instant thin-layer chromatography at a specific activity of 0.4 MBq/μg.

In vitro studies

For *in vitro* studies a murine fibroblast cell line, 3T3, stably transfected with murine FAP [3T3-FAP (a kind gift from Roche, Basel, Switzerland)] was cultured in DMEM with 10% foetal calf serum, penicillin, streptomycin and

1.5 μg/ml puromycin at 37°C and 5% carbon dioxide (CO_2) [13]. Since conjugation of multiple IRDye700DX molecules may affect binding capacity, the immunoreactive fraction of the antibody–PS conjugate was determined through a Lindmo assay [22]. Briefly, 20 000 cpm [^{111}In]In-DTPA-28H1-700DX per vial (corresponding to 14.5 ng and 15.9 ng antibody-conjugate for SR 1.2 and 3, respectively) were added to a serial dilution of 3T3-FAP cells and incubated for 1 h at 37°C with 5% CO_2. The specificity of the binding was evaluated by adding an excess of 5 μg unlabelled antibody.

In vitro photodynamic therapy

For *in vitro* tPDT 1×10^5 3T3-FAP cells were seeded in 24-well plates. After overnight culture to ensure cell adherence, the cells were incubated with 0.5 μg/ml DTPA-28H1-700DX in binding buffer [DMEM with 0.5% BSA (Sigma-Aldrich, St. Louis, MO, USA) (BB)] for 4 h at 37°C. Control cells were incubated with DTPA-28H1, a control antibody conjugated with IRDye700DX (hMN-14-700DX, not specific for FAP) or BB alone, as indicated in the figures. After incubation, the cells were washed and exposed to 690 nm light from a light-emitting diode light source (LEDfactory, Leeuwarden, The Netherlands) [23]. After light exposure, the cells were incubated for 1 h at 37°C. The medium was subsequently removed and CellTiter-Glo (Promega, Madison, WI, USA) was used to measure adenosine triphosphate levels. Cell viability was expressed as the mean percentage of luminescence compared with the non-exposed BB control group.

Animal experiments

AIA

AIA was induced in female C57Bl/6NRj mice. At day−21 the mice were immunized through a s.c. injection of 100 μg methylated BSA (mBSA; Sigma-Aldrich) emulsified in 100 μl Freund's complete adjuvant (FCA; Difco Laboratories, Detroit, MI, USA) on the shoulders. Additionally, an IP injection of heat-killed *Bordetella pertussis* (4×10^7 cells/mouse; National Institute for Public Health and the Environment, Bilthoven, The Netherlands) in 200 μl saline (0.9% NaCl) was administered. At day−14 the immunization and *Bordetella* injection were repeated. On day0, arthritis was induced through an IA injection of 60 μg mBSA in 6 μl PBS into the knee joint.

CIA

CIA was induced in male DBA/1JRj mice as described previously [24]. The mice received two injections of 100 μg bovine collagen type II (Radboud University Medical Center in-house production, batch 03-04-08). The first dose was emulsified in FCA and administered intradermally at the base of the tail. The second dose was administered in PBS intraperitoneally at day 21. Mice subsequently spontaneously developed arthritis around day 21–25. Mice were scored three times a week for the development of arthritis in each paw according to a 2-point scale of swelling and redness as

described previously [13]. Mice with a score ≥0.5 in one of the hind paws were included in the study.

Biodistribution

Biodistribution analysis of the [^{111}In]In-DTPA-28H1-700DX compound was performed in healthy, treatment-naïve, male C57BL/6NRj mice and female C57BL/6NRj mice with AIA using different SRs of the antibody. The [^{111}In]In-DTPA-28H1 conjugate was used as a control. All conjugates were labelled with 0.4–0.6 MBq [^{111}In]InCl$_3$ for a dose of 50 μg protein in 200 μl PBS. Biodistribution of the compounds was determined after 24 h by resecting and weighing tissues of interest and subsequently determining tissue uptake of ^{111}In using a gamma counter (WIZARD, 2480 Automatic Gamma Counter, Perkin Elmer, Waltham, MA, USA). After determining the optimal SR, we determined the optimal time for tPDT. Biodistribution was determined 4, 12, 24 or 72 h after injection. Knee joints were stored in 4% formalin and embedded in paraffin for histological analysis. Haematoxylin and eosin staining was performed on 7 μm thick slices and the level of inflammation was assessed.

In a subset of animals ($n = 3$/group) SPECT/CT images were acquired using a U-SPECT/CT-II (MILabs, Utrecht, The Netherlands). Animals were injected with 50 μg, 15–17 MBq [^{111}In]In-DTPA-28H1 with or without IRDye700DX and scanned for 60 min (4×15 min frames) using a 1 mm diameter pinhole ultra-high-sensitivity mouse collimator. SPECT scans were followed by CT scans (65 kV, 615 μA). The SPECT scans were reconstructed using software from MILabs using a 0.2 mm voxel size, one iteration and 16 subsets.

Photodynamic therapy

Ex vivo tPDT was performed in the isolated knee joints of mice with bilateral AIA. At day 4 after arthritis onset, the animals were injected with 50 μg DTPA-28H1-700DX (SR 2.5) in 200 μl PBS. After 24 h the mice were sacrificed and the paws were removed. Next, the joints were fixed on a custom board, the left hind paws were shielded using aluminium foil to mimic the real treatment situation and the right hind paws were exposed to 35.2 J/cm^2 of 690 nm light. After treatment, the remaining fluorescent signal of the PS was visualized using a fluorescence camera system (IVIS Lumina; PerkinElmer, Waltham, MA, USA) with an excitation filter (640 nm) and an emission filter (Cy5.5, 1 min acquisition). Data were corrected for autofluorescence and quantified using a standard region of interest. The maximum fluorescence intensity from the region of interest was subsequently normalized for the shielded, non-exposed group.

In vivo tPDT was performed in mice with CIA after the development of visible arthritis (score ≥0.5) in the hind paws of the mice. After inclusion, the mice were injected intravenously with 50 μg DTPA-28H1-700DX (SR 2.5) in 200 μl PBS or with PBS only as a control and after 24 h one inflamed hind paw was exposed to 17.6 or 52 J/cm^2 of 690 nm light. The PBS group was exposed to the highest light dose. Development of arthritis was scored three times a week by a blinded observer. Mice were

sacrificed at the end of the study or when they reached the predefined humane endpoint of a cumulative arthritis score ≥7.

Statistical analysis

Results are presented as mean (s.d.). Statistical significance was tested using unpaired Student's *t* test or one- or two-way analysis of variance in GraphPad Prism software (version 5.03; GraphPad Software, San Diego, CA, USA). Normal distribution was tested using the Kolmogorov–Smirnov test. Samples were normally distributed unless stated otherwise. A *P*-value <0.05 was considered significant.

Results

The immunoreactive fraction is not significantly impacted by PS conjugation

The immunoreactive fraction of 28H1-700DX was determined for two different SRs of IRDye-700DX. These were 94.7% for a 28H1-700DX conjugate with SR 1.2 and 92.5% for a conjugate with SR 3. These immunoreactive fraction values are comparable to those previously described for the DTPA-28H1 construct without IRDye700DX [10].

Targeted photodynamic therapy selectively induces cytotoxicity in FAP+ fibroblasts *in vitro*

Almost 90% cell death was achieved *in vitro* when the 3T3-FAP cells were subjected to the anti-FAP antibody and 17.6 J/cm^2 radiant exposure, irrespective of the SRs [SR 1.2, 89% (s.d. 4) and SR 3, 89% (s.d. 3); *P* < 0.001 (Fig. 1A)]. At a light dose of 2.9 J/cm^2, we observed a significant difference in cell killing between the different constructs: SR 1.2 caused only moderate cell killing [18% (s.d. 9), *P* < 0.05], whereas FAP-tPDT with 28H1-700DX SR 3 caused more pronounced cell killing [52% (s.d. 10), *P* < 0.001]. Cell viability was not significantly reduced for any of the radiant exposures when the cells were only exposed to the light without the antibody, nor

when they were incubated with a control antibody conjugated to the same photosensitizer. This indicates that FAP-tPDT is able to specifically and efficiently kill 3T3-FAP cells.

In contrast to the substantial tPDT-induced cell death in FAP-positive fibroblasts, cell viability of 3T3 fibroblasts that were not transfected with FAP (control group) did not decrease upon incubation with the 28H1-700DX construct in combination with subsequent exposure to 690 nm light (Fig. 1B).

Tracer uptake in the arthritic knee joint is unaffected by IRDye-700DX conjugation to 28H1

Since the *in vitro* study demonstrated that tPDT was more effective when a higher SR is used, we assessed the biodistribution of the tracer with SRs >1.2 (SR of 2.3 and 6.5) in naïve C57BL/6NRj mice. In most of the organs, the accumulation of [111In]In-DTPA-28H1 with or without 700DX was similar, with the exception of the liver, spleen, lung, knee joints and blood (Fig. 2A and B). Conjugation of the PS to the anti-FAP-antibody significantly increased the liver, spleen and knee joint uptake and decreased lung and blood levels. Tracer uptake in the bone marrow was not significantly different between the conjugates.

Since an SR of 2.3 resulted in lower tracer accumulation in the liver and higher blood levels compared with an SR of 6.5, the subsequent studies were performed with an [111In]In-DTPA-28H1-700DX conjugate with an SR of 2.2–2.5. New antibody conjugation for these studies yielded an SR of 2.5. With this conjugate, we investigated the biodistribution at 4, 12, 24 and 72 h after injection in mice with AIA (Fig. 3A). There was rapid blood clearance with only 1.0%ID/g (s.d. 0.1) remaining in the circulation after 72 h. Liver uptake of the tracer peaked at 12 h with a mean uptake of 37.0 %ID/g (s.d. 2.6) and decreased over time [24 h: 26.8 %ID/g (s.d. 3.4), 72 h: 23.9 (1.9), *P* < 0.001]. Tracer uptake in the inflamed knee joint did not vary significantly between 4, 12 and 24 h post-injection, but it was significantly lower 72 h post-injection when compared with the uptake at 12 and 24 h [4 h: 2.4 %ID (s.d. 0.4), 12 h: 2.7 (0.4), 24 h:

Fig. 1 Photodynamic therapy performed on 3T3 cells transfected with FAP and non-transfected cells
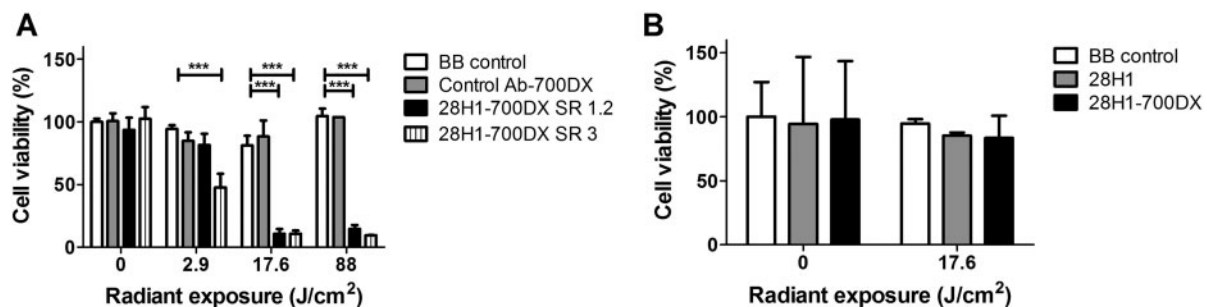
Cell death is only observed when the cells expressing FAP are incubated with the 28H1-700DX construct and are exposed to light. With light exposures of 88 J/cm^2, a maximum cell death of 90.49% (s.d. 0.23) can be achieved (*n* = 3). One-way analysis of variance with Bonferroni post-test. ***P* < 0.001.

FIG. 2 Biodistribution of [^{111}In]In-DTPA-28H1 and [^{111}In]In-DTPA-28H1-IRDye700DX with SR 2.3 or 6.5
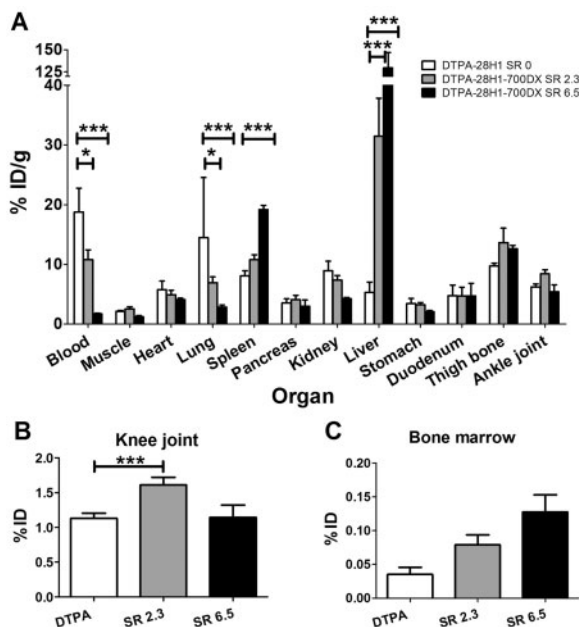
(**A**) Biodistribution of the DTPA-28H1-700DX conjugate is different compared with DTPA-28H1, with most strikingly with a higher liver accumulation. (**B**) Tracer accumulation in the knee joint is not negatively affected by conjugation to the PS. (**C**) Tracer uptake in the bone marrow seems to increase, but this was not statistically significant. Data are shown as mean (S.D.). Two-way analysis of variance with Bonferroni post-test. *$P < 0.05$, ***$P < 0.001$; $n = 5$ mice/group.

2.7 (0.6), 72 h: 2.1 (0.3), $P < 0.01$ and $P < 0.05$ for 72 h compared with 12 h and 24 h post-injection, respectively (Fig. 3B)]. Uptake in the inflamed joint was 3.3-fold higher than in the non-inflamed joint ($P < 0.001$ for all time points). SPECT images acquired at these time points reflect the uptake pattern observed in the biodistribution, with clear FAP targeting in the arthritic joint and no discernible signal in the contralateral, unaffected joint (Fig. 3C).

Correlation of tracer uptake (%ID) in the inflamed knee joint with the histological score of inflammation shows a significant correlation 24 and 72 h after injection of the tracer [24 h: $r^2 = 0.77$ ($P = 0.02$), 72 h: $r^2 = 0.88$ ($P = 0.006$)].

Photodynamic therapy *ex vivo and in vivo*

Next, we assessed whether locally applied light can efficiently excite the 28H1-700DX conjugate in inflamed knee joints of female mice with AIA. The mice were sacrificed 24 h after i.v. injection of the conjugate and joints were *ex vivo* exposed to light to activate the PS. Fluorescent imaging of the PS before light exposure showed no differences in initial signal intensity between the later exposed and non-exposed inflamed knee joints

(Fig. 4A). After 35.2 J/cm^2 radiant exposure, the fluorescent signal decreased strikingly in the exposed knee joints [percentage decrease in fluorescent intensity was 79.4% (S.D. 3.0) *vs* 28.5% (S.D. 7.5) in exposed and shielded joints compared with baseline, respectively; $P < 0.01$ (Fig. 4B)]. The decrease in fluorescent signal of the dye in the inflamed knee joints indicates successful photostimulation and subsequent bleaching of the PS.

Finally, the therapeutic effect of FAP-tPDT was evaluated in male DBA/1JRj mice with CIA. In this proof-of-concept study, one inflamed hind paw was treated with light 24 h after injection of the conjugate. The development of arthritis was ameliorated in both the 8.8 and 26.4 J/cm^2 tPDT-treated groups (area under the curve of the first two time points of arthritis development was 3.5 (S.D. 1.3), 2.0 (S.D. 1.1) and 1.9 (S.D. 1.4) for the PBS control, 8.8 and 26.4 J/cm^2 treated groups, respectively; $P < 0.05$ (Fig. 5)]. After this initial delay in arthritis in the treated paws, no differences in arthritis scores were observed in the later time points. Consequently, the area under the curve was also no longer significantly different between the control and treatment groups.
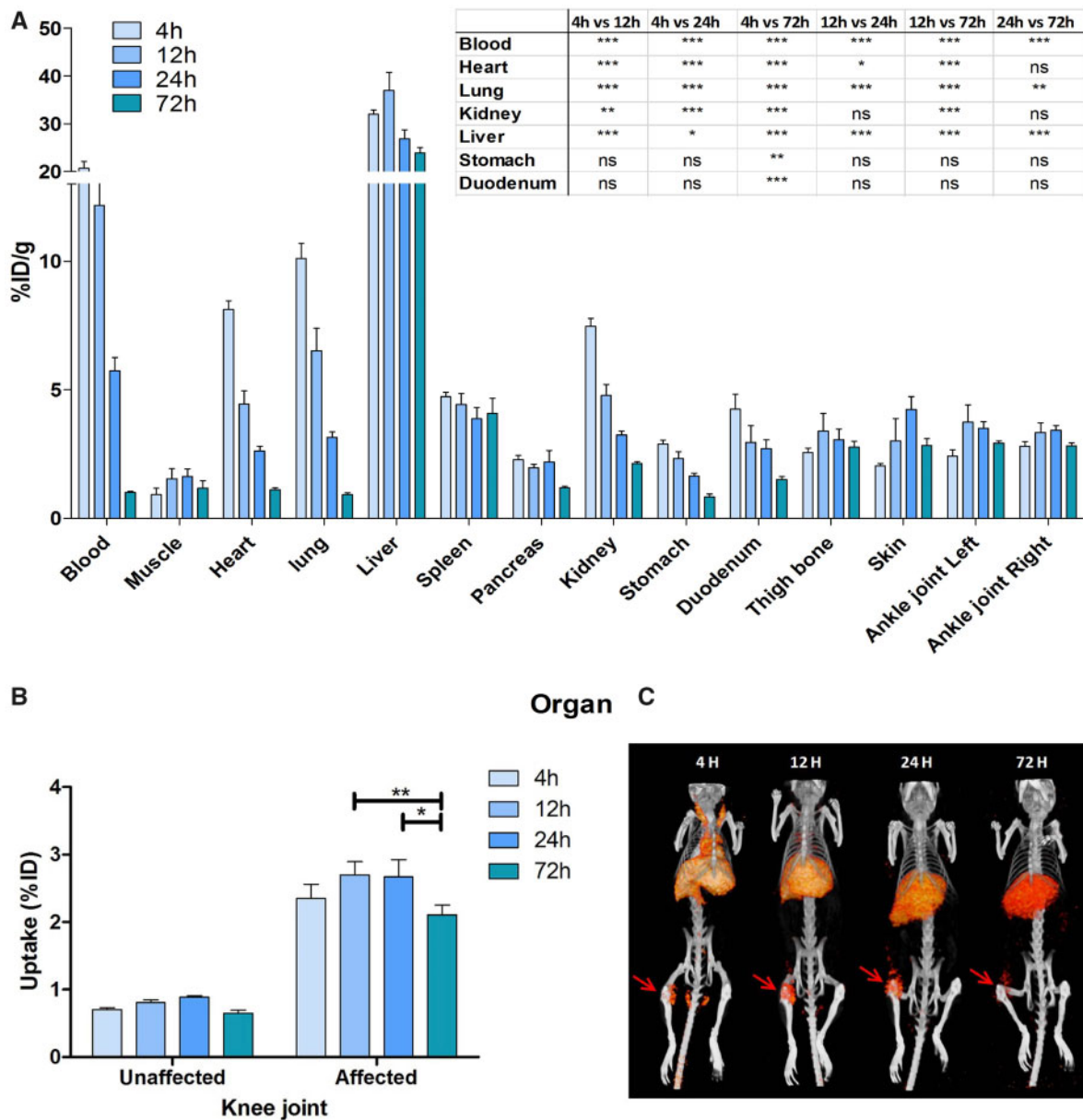
Discussion

Here we demonstrate the feasibility of using FAP-tPDT to deplete FAP$^+$ SFs both *in vitro* and *in vivo* in a CIA mouse model of arthritis. Conjugation of the PS to 28H1 and subsequent tPDT allowed specific depletion of FAP-expressing fibroblasts as determined by *in vitro* tPDT performed on 3T3 cells transfected with FAP. Photobleaching, and thus activation of the PS, was demonstrated after *ex vivo* FAP-tPDT in arthritic knee joints of AIA mice injected with the 28H1-700DX conjugate. Finally, FAP-tPDT resulted in an amelioration of arthritis development in CIA, showing the potential of this therapy.

An important percentage of patients initially fail to respond to first-line biologic DMARD (bDMARD) treatment. Buch *et al.* [3] commented that 20% of patients even fail to respond to second-line bDMARDs. Current bDMARDs interfere with the inflammatory processes occurring during RA and since the disease is very heterogeneous, with different immune cell populations driving disease in different patients, it is not surprising that bDMARD therapy is not effective in all patients. By instead focussing the treatment on the aberrant synovial cells, treatment can be administered independent of the immunological drivers of disease in the individual patients. It has already been demonstrated that high FAP expression is a hallmark of affected synovium in RA patients and is therefore an excellent candidate for tPDT [10, 16]. Treatment with FAP-tPDT can be administered repeatedly and, by adapting the light dose delivered, can also be individualized.

We demonstrate that with our FAP-targeted approach, the accumulation in off-target tissues is negligible, thus limiting the side effects of tPDT. The use of untargeted photodynamic therapy has previously been described in

Fig. 3 Biodistribution of [^{111}In]In-DTPA-28H1-IRDye700DX at different time points in mice with AIA

|	4h vs 12h	4h vs 24h	4h vs 72h	12h vs 24h	12h vs 72h	24h vs 72h
Blood	***	***	***	***	***	***
Heart	***	***	***	*	***	ns
Lung	***	***	***	***	***	**
Kidney	**	***	***	ns	***	ns
Liver	***	*	***	***	***	***
Stomach	ns	ns	**	ns	ns	ns
Duodenum	ns	ns	***	ns	ns	ns

(**A**) The tracer shows rapid clearance from the blood. (**B**) Tracer accumulation is higher in the arthritic knee joint than in the contralateral joint ($P < 0.001$ for all time points). (**C**) SPECT/CT imaging shows the same pattern as the biodistribution data, with high uptake in the inflamed right knee joint (red arrow) and the liver. Data are shown as mean (s.d.). Two-way analysis of variance with Bonferroni post-test. *$P < 0.05$, **$P < 0.01$, ***$P < 0.001$; $n = 5$ mice/group.

experimental models of arthritis using PS alone or liposomes loaded with PS [25–28]. However, the authors report significant side effects as a consequence of the accumulation of PS in off-target tissues such as muscle. Further tailoring the therapy to subsets of cells critical in RA, through the use of specific targeting molecules, could minimize these effects.

The penetration depth of light in biological tissue as well as lipophilicity and the photostability of the PS are important factors determining the success of tPDT. Using a PS excited at a higher (near infrared) wavelength might increase the therapeutic effect due to greater tissue penetration. The excitation of IRDye700DX at 690 nm offers this advantage, penetrating ~60% deeper in the tissue than light of 550 nm, at which, for example, TSPP-TiO2 is excited [29]. Light penetration depth is also an important consideration when selecting joints suitable for treatment. Even though the 690 nm light at which IRDye700DX is excited is suitable for treatment of smaller joints, such as the interphalangeal joints, larger joints may

FIG. 4 Fluorescence imaging of 28H1-700DX in arthritic knee joints after PDT *ex vivo*
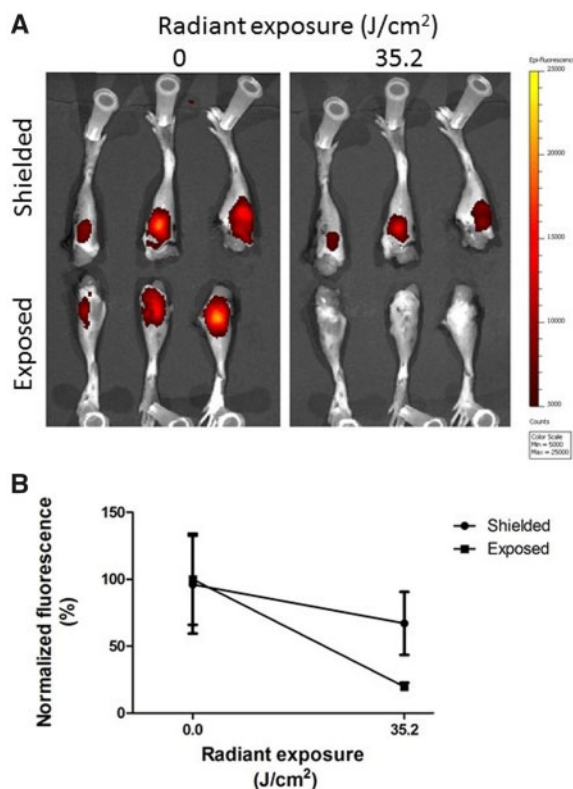
(**A**) Images of fluorescence observed at baseline and after 35.2 J/cm² radiant exposure. (**B**) Quantification of mean fluorescent intensity normalized to baseline. Quantification of the fluorescent signal shows a faster decrease in the knee joints that were exposed to light when compared with the shielded group ($P < 0.01$). Data are shown as mean (S.D.). $n = 3$ mice/group.

be too big for efficient treatment. Endoscopically delivering the light might overcome this hurdle.

Conjugation of the PS to the anti-FAP antibody did not change the efficient accumulation of the construct in inflamed joints. However, it did change its accumulation in the liver, which was increased, and this was accompanied by faster blood clearance. With increasing SRs, this effect became more pronounced, similar to other related tracers conjugated with fluorophores [30]. The observed differences may be explained by the change in charge and increased lipophilicity of the antibody conjugate [31]. Higher liver uptake resulted in lower levels in the surrounding tissue, which might beneficially impact therapy results, since fewer bystander effects can be expected.

To further limit damage to surrounding tissue, adequate shielding is crucial. This is exemplified by the decrease in fluorescence observed in the contralateral shielded joint in the *ex vivo* tPDT experiment. The observed reduction may be explained by incomplete or ineffective shielding of those joints in our experimental

FIG. 5 Development of collagen-induced arthritis after FAP-tPDT
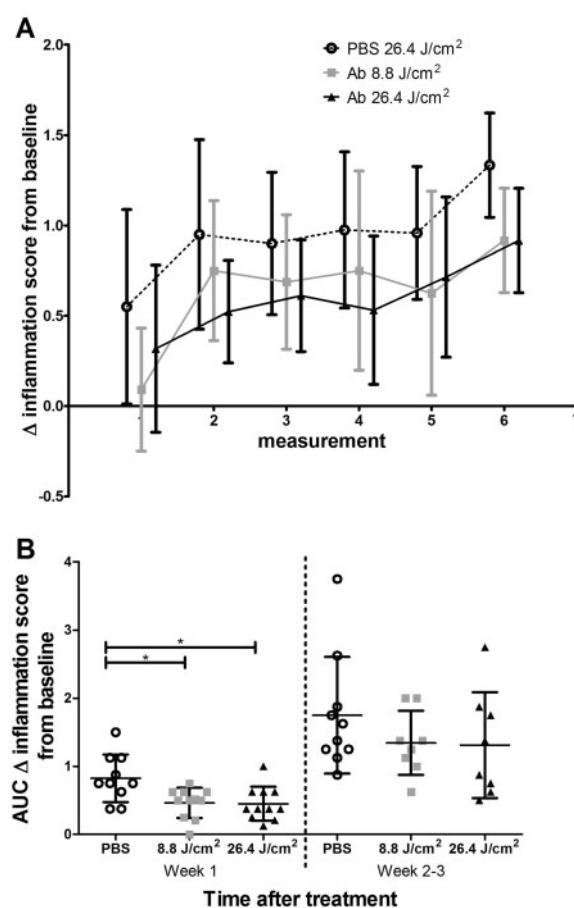
(**A**) Change in inflammation score compared with baseline. (**B**) Area under the curve of the change in inflammation compared with baseline for the first two measurements and the later time points. Data are shown as mean (S.D.). $n = 11$ mice at baseline.

setup, indicating that shielding should be very carefully controlled during treatment. Using lasers will allow for more focussed and targeted light and may be more feasible in practice.

The recurrence of arthritis in the treated joint in the CIA model might be attributed to the systemic nature of this mouse model. Following temporary improvement of the inflammation, the circulating pro-inflammatory mediators driving CIA overcame the therapeutic effect. In clinical practice, the FAP-tPDT could be repeated when this occurs. This is not possible in mice, since repeated injections cause more rapid clearance of the construct due to recognition by the immune system.

In conclusion, we have demonstrated the feasibility of FAP-tPDT in arthritis therapy. FAP^{+} fibroblasts can be efficiently depleted using this therapy, resulting in an amelioration of the disease. Future research should focus on discerning the therapeutic value of this

approach through monitoring the development of arthritis in animal models of the disease. Toxicity and safety studies will have to be performed before clinical translation can be considered.

Acknowledgements

Disclosure statement: CK declares employment, patents and stock ownership with Roche. The other authors have declared no conflicts of interest.

References

1 Silman AJ, Pearson JE. Epidemiology and genetics of rheumatoid arthritis. Arthritis Res 2002;4:S265–72.

2 Smolen JS, Aletaha D, McInnes IB. Rheumatoid arthritis. Lancet 2016;388:2023–38.

3 Buch MH. Defining refractory rheumatoid arthritis. Ann Rheum Dis 2018;77:966–9.

4 Bottini N, Firestein GS. Duality of fibroblast-like synoviocytes in RA: passive responders and imprinted aggressors. Nat Rev Rheumatol 2013;9:24–33.

5 Bartok B, Firestein GS. Fibroblast-like synoviocytes: key effector cells in rheumatoid arthritis. Immunol Rev 2010; 233:233–55.

6 Filer A. The fibroblast as a therapeutic target in rheumatoid arthritis. Curr Opin Pharmacol 2013;13: 413–9.

7 Pap T, Muller-Ladner U, Gay RE, Gay S. Fibroblast biology: role of synovial fibroblasts in the pathogenesis of rheumatoid arthritis. Arthritis Res 2000;2:361–7.

8 Turner JD, Filer A. The role of the synovial fibroblast in rheumatoid arthritis pathogenesis. Curr Opin Rheumatol 2015;27:175–82.

9 Mizoguchi F, Slowikowski K, Wei K *et al*. Functionally distinct disease-associated fibroblast subsets in rheumatoid arthritis. Nat Commun 2018;9:789.

10 Croft AP, Campos J, Jansen K *et al*. Distinct fibroblast subsets drive inflammation and damage in arthritis. Nature 2019;570:246–51.

11 Bauer S, Jendro MC, Wadle A *et al*. Fibroblast activation protein is expressed by rheumatoid myofibroblast-like synoviocytes. Arthritis Res Ther 2006;8:R171.

12 Scanlan MJ, Raj BK, Calvo B *et al*. Molecular cloning of fibroblast activation protein alpha, a member of the serine protease family selectively expressed in stromal fibroblasts of epithelial cancers. Proc Natl Acad Sci USA 1994;91:5657–61.

13 Laverman P, van der Geest T, Terry SY *et al*. Immuno-PET and immuno-SPECT of rheumatoid arthritis with radiolabeled anti-fibroblast activation protein antibody correlates with severity of arthritis. J Nucl Med 2015;56: 778–83.

14 van der Geest T, Laverman P, Gerrits D *et al*. Liposomal treatment of experimental arthritis can be monitored noninvasively with a radiolabeled anti-fibroblast activation protein antibody. J Nucl Med 2017; 58:151–5.

15 Waldele S, Koers-Wunrau C, Beckmann D *et al*. Deficiency of fibroblast activation protein alpha ameliorates cartilage destruction in inflammatory destructive arthritis. Arthritis Res Ther 2015;17:12.

16 Dakin SG, Coles M, Sherlock JP *et al*. Pathogenic stromal cells as therapeutic targets in joint inflammation. Nat Rev Rheumatol 2018;14:714–26.

17 Mallidi S, Anbil S, Bulin AL *et al*. Beyond the barriers of light penetration: strategies, perspectives and possibilities for photodynamic therapy. Theranostics 2016;6:2458–87.

18 van Straten D, Mashayekhi V, de Bruijn HS, Oliveira S, Robinson DJ. Oncologic photodynamic therapy: basic principles, current clinical status and future directions. Cancers (Basel) 2017;9:19.

19 Brünker P, Wartha K, Friess T *et al*. RG7386, a novel tetravalent FAP-DR5 antibody, effectively triggers FAP-dependent, avidity-driven DR5 hyperclustering and tumor cell apoptosis. Mol Cancer Ther 2016;15: 946–57.

20 Schlothauer T, Herter S, Koller CF *et al*. Novel human IgG1 and IgG4 Fc-engineered antibodies with completely abolished immune effector functions. Protein Eng Des Sel 2016;29:457–66.

21 Brom M, Joosten L, Oyen WJ, Gotthardt M, Boerman OC. Improved labelling of DTPA- and DOTA-conjugated peptides and antibodies with 111In in HEPES and MES buffer. EJNMMI Res 2012;2:4.

22 Lindmo T, Boven E, Cuttitta F, Fedorko J, Bunn PA Jr. Determination of the immunoreactive fraction of radiolabeled monoclonal antibodies by linear extrapolation to binding at infinite antigen excess. J Immunol Methods 1984;72:77–89.

23 de Boer E, Warram JM, Hartmans E *et al*. A standardized light-emitting diode device for photoimmunotherapy. J Nucl Med 2014;55:1893–8.

24 Joosten LAB, Lubberts E, Durez P *et al*. Role of interleukin-4 and interleukin-10 in murine collagen-induced arthritis. Protective effect of interleukin-4 and interleukin-10 treatment on cartilage destruction. Arthritis Rheum 1997;40:249–60.

25 Lu Y, Li L, Lin Z *et al*. A new treatment modality for rheumatoid arthritis: combined photothermal and photodynamic therapy using Cu7.2 S4 nanoparticles. Adv Healthc Mater 2018;7:e1800013.

26 Zhao C, Ur Rehman F, Yang Y *et al*. Bio-imaging and photodynamic therapy with tetra sulphonatophenyl porphyrin (TSPP)-TiO_2 nanowhiskers: new approaches in rheumatoid arthritis theranostics. Sci Rep 2015;5: 11518.

27 Funke B, Jungel A, Schastak S *et al*. Transdermal photodynamic therapy—a treatment option for rheumatic destruction of small joints? Lasers Surg Med 2006;38: 866–74.

28 Hansch A, Frey O, Gajda M *et al*. Photodynamic treatment as a novel approach in the therapy of arthritic joints. Lasers Surg Med 2008;40:265–72.

29 Ash C, Dubec M, Donne K, Bashford T. Effect of wavelength and beam width on penetration in light-tissue interaction using computational methods. Lasers Med Sci 2017;32:1909–18.

30 Rijpkema M, Bos DL, Cornelissen AS *et al*. Optimization of dual-labeled antibodies for targeted intraoperative imaging of tumors. Mol Imaging 2015;14:348–55.

31 Boswell CA, Tesar DB, Mukhyala K *et al*. Effects of charge on antibody tissue distribution and pharmacokinetics. Bioconjug Chem 2010;21: 2153–63.